16. Wide-Bandgap II–VI Semiconductors: Growth and Properties

Wide-bandgap II–VI compounds are been applied to optoelectronic devices, especially light-emitting devices in the short-wavelength region of visible light, because of their direct gap and suitable bandgap energies. Many methods have been extensively applied to grow high-quality films and bulk single crystals from the vapor and liquid phases.

This chapter firstly discusses the basic properties and phase diagrams of wide-bandgap II–VI compounds such as ZnS, ZnO, ZnSe, ZnTe, CdSe and CdTe. Then the growth methods and recent progress in films and bulk crystal growth are reviewed. In the epitaxial growth methods, the focus is on liquid-phase epitaxy (LPE), vapor-phase epitaxy (VPE) containing conventional VPE, hot-wall epitaxy (HWE), metalorganic chemical vapor deposition (MOCVD) or metalorganic phase epitaxy (MOVPE), molecular-beam epitaxy (MBE) and atomic-layer epitaxy (ALE). In bulk crystal growth, two typical growth methods, chemical/physical vapor transport (CVT/PVT) and Bridgman techniques, are introduced.

16.1 **Crystal Properties** ... 6
16.1.1 Basic Properties ... 6
16.1.2 Phase Diagram ... 6

16.2 **Epitaxial Growth** ... 6
16.2.1 The LPE Technique ... 6
16.2.2 Vapor-Phase Epitaxy Techniques. 6

16.3 **Bulk Crystal Growth** ... 11
16.3.1 The CVT and PVT Techniques ... 11
16.3.2 Hydrothermal Growth ... 13
16.3.3 Bridgman and Gradient Freezing (GF) Method ... 14
16.3.4 The Traveling Heater Method (THM) ... 16
16.3.5 Other Methods ... 16

16.4 **Conclusions** ... 17

References ... 17

Wide-bandgap II–VI compounds are expected to be one of the most vital materials for high-performance optoelectronics devices such as light-emitting diodes (LEDs) and laser diodes (LDs) operating in the blue or ultraviolet spectral range. Additionally, the high ionicity of these compounds makes them good candidates for high electro-optical and electromechanical coupling. The basic promises of wide-bandgap materials can be found in Fig. 16.1.

Thin films were commonly grown using the conventional vapor-phase epitaxy (VPE) method for 60 s. With the development of science and technology, new and higher requirements arose for material preparation. For this reason, novel epitaxial growth techniques were developed, including hot-wall epitaxy (HWE) [16.1], metalorganic chemical vapor deposition (MOCVD) [16.2], molecular-beam epitaxy (MBE) [16.3], metalorganic molecular-beam epitaxy (MOMBE) [16.4] and atomic-layer epitaxy (ALE) [16.5]. Using these growth methods, film thickness can be controlled, and quality can be improved.

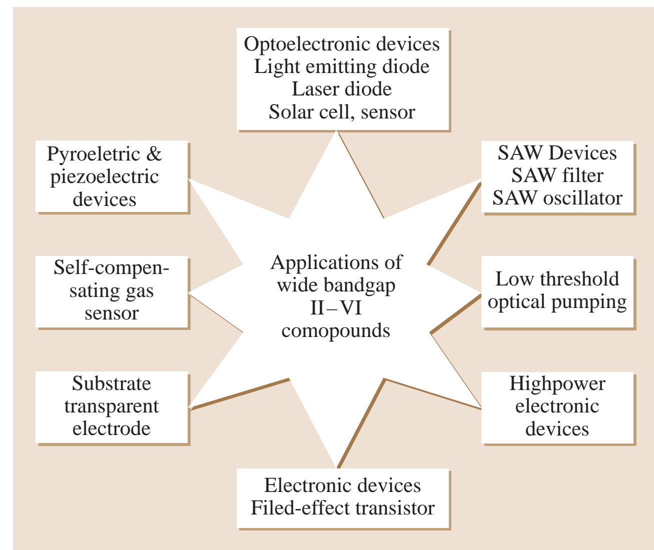

Fig. 16.1 Application of II–VI wide-bandgap compounds

Table 16.1 Properties of some wide-bandgap II–VI compound semiconductors

Material Property	ZnS	ZnO	ZnSe	ZnTe	CdS	CdSe	CdTe
Melting point (K)	2038 (WZ, 150 atm)	2248	1797	1513	2023 (WZ, 100 atm)	1623	1370 (ZB)
Energy gap E_g at 300 K (eV)(ZB*/WZ*)	3.68/3.911	–/3.4	2.71/–	2.394	2.50/2.50	–/1.751	1.475
dE_g/dT ($\times 10^{-4}$ eV/K) ZB/WZ	4.6/8.5	–/9.5	4.0/–	5.5/–	–/5.2	–/4.6	5.4/–
Structure	ZB/WZ	WZ	ZB/WZ	ZB	WZ	WZ	ZB
Bond length (µm)	2.342 (WZ)	1.977 (WZ)	2.454 (ZB)	2.636 (ZB)	2.530 (ZB)	2.630 (ZB)	2.806 (ZB)
Lattice constant (ZB) a_0 at 300 K (nm)	0.541	–	0.567	0.610	0.582	0.608	0.648
ZB nearest-neighbor dist. at 300 K (nm)	0.234	–	0.246	0.264	0.252	0.263	0.281
ZB density at 300 K (g/cm^3)	4.11	–	5.26	5.65	4.87	5.655	5.86
Lattice constant (WZ) at 300 K (nm)							
$a_0 = b_0$	0.3811	0.32495	0.398	0.427	0.4135	0.430	–
c_0	0.6234	0.52069	0.653	0.699	0.6749	0.702	–
c_0/a_0	1.636	1.602	1.641	1.637	1.632	1.633	–
WZ density at 300 K (g/cm^3)	3.98	5.606	–	–	4.82	5.81	–
Symmetry ZB/WZ	C6me/F43m	–/C6me	–/F43m	–/F43m	C6me/F43m	C6me/F43m	–/–
Electron affinity χ (eV)			4.09	3.53	4.79	4.95	4.28
Stable phase(s) at 300 K	ZB & WZ	WZ	ZB	ZB	ZB & WZ	ZB & WZ	ZB
Solid–solid phase transition temperature (K)	1293	–	1698	–	–	403	1273(?)
Heat of crystallization ΔH_{LS} (kJ/mol)	44	62	52	56	58	45	57
Heat capacity C_P (cal/mol K)	11.0	9.6	12.4	11.9	13.2	11.8	–
Ionicity (%)	62	62	63	61	69	70	72
Equilibrium pressure at c.m.p. (atm)	3.7	–	1.0	1.9	3.8	1.0	0.7
Minimum pressure at m.p. (atm)	2.8	7.82	0.53	0.64	2.2	0.4–0.5	0.23
Specific heat capacity (J/gK)	0.469	–	0.339	0.16	0.47	0.49	0.21
Thermal conductivity (W cm^{-1}K^{-1})	0.27	0.6	0.19	0.18	0.2	0.09	0.01
Thermo-optical cofficient $(dn/dT)(\lambda = 10.6\,\mu m)$	4.7	–	6.1	–	–	–	11.0
Electrooptical coefficient r_{41} (m/V) ($\lambda = 10.6\,\mu m$)	2×10^{-12}	–	2.2×10^{-12}	4.0×10^{-12} ($r_{41} = r_{52} = r_{63}$)	–	–	6.8×10^{-12}
Linear expansion coefficient (10^{-6} K^{-1}) ZB/WZ	–/6.9	2.9/7.2	7.6/–	8.0/–	3.0/4.5	3.0/7.3	5.1/–
Poisson ratio	0.27		0.28				0.41
Dielectric constant $\varepsilon_0/\varepsilon_\infty$	8.6/5.2	8.65/4.0	9.2/5.8	9.3/6.9	8.6/5.3	9.5/6.2	2.27/–
Refractive index ZB/WZ	2.368/2.378	–/2.029	2.5/–	2.72/–	–/2.529	2.5/–	2.72/–

m.p. – melting point; c.m.p. – congruent melting point; ZB – zinc blende; WZ – wurtzite

Table 16.1 (continued)

Material Property	ZnS	ZnO	ZnSe	ZnTe	CdS	CdSe	CdTe
Absorption coeff. (including two surfaces) ($\lambda = 10.6\,\mu$m)(cm^{-1})	≤ 0.15	–	$1-2\times10^{-3}$	–	≤ 0.007	≤ 0.0015	≤ 0.003
Electron effective mass (m^*/m_0)	–0.40	–0.27	0.21	0.2	0.21	0.13	0.11
Hole effective mass m^*_{dos}/m_0	–	–	0.6	circa 0.2	0.8	0.45	0.35
Electron Hall mobility (300) K for $n =$ lowish (cm^2/Vs)	165	125	500	340	340	650	1050
Hole Hall mobility at 300 K for $p =$ lowish (cm^2/Vs)	5	–	30	100	340	–	100
Exciton binding energy (meV)	36	60	21	10	30.5	15	12
Average phonon energy (meV) ZB/WZ	16.1/17.1	–	15.1/–	10.8/–	–/13.9	18.9/25.4	5.8/–
Elastic constant (10^{10} N/m^2)							
C_{11}	1.01±0.05	–	8.10±0.52	0.72±0.01	–	–	5.57
C_{12}	0.64±0.05	–	4.88±0.49	0.48±0.002	–	–	3.84
C_{44}	0.42±0.04	–	4.41±0.13	0.31±0.002	–	–	2.095
Knoop hardness (N/cm^2)	0.18	0.5	0.15	0.13	–	–	0.10
Young's modulus	10.8 Mpsi	–	10.2 Mpsi	–	45 GPa	5×10^{11} dyne/cm^2	3.7×10^{11} dyne/cm^2

m.p. – melting point; c.m.p. – congruent melting point; ZB – zinc blende; WZ – wurtzite

On the other hand, basic research work into growing bulk crystals of wide-bandgap II–VI compounds has been carried out. Focus was put on high-purity, high-quality, large single crystals [16.6–10]. Since the electrical and optical properties of semiconductor compounds are drastically affected by impurities and native defects, purity and quality are very important for fundamental research and engineering application where they are used as substrates. Bulk single crystals of these wide-bandgap II–VI compounds have been grown from the vapor, liquid and solid phases. Vapor-phase growth includes chemical vapor transport (CVT) and physical vapor transport (PVT) methods; liquid-phase methods includes growth from the melt or solvent. Among these growth methods, melt growth is most suitable to produce sizable bulk crystals for relatively short growth duration. Growth methods for films and bulk crystals of wide-bandgap II–VI compounds are summarized in Fig. 16.2 and the details can be found in Sects. 16.2 and 16.3.

This chapter firstly describes the physical and chemical properties of these wide-bandgap II–VI compounds, then reviews the growth techniques and introduces the main results in preparing film and bulk single crystals of ZnS, ZnO, ZnSe, ZnTe, CdTe, and so on.

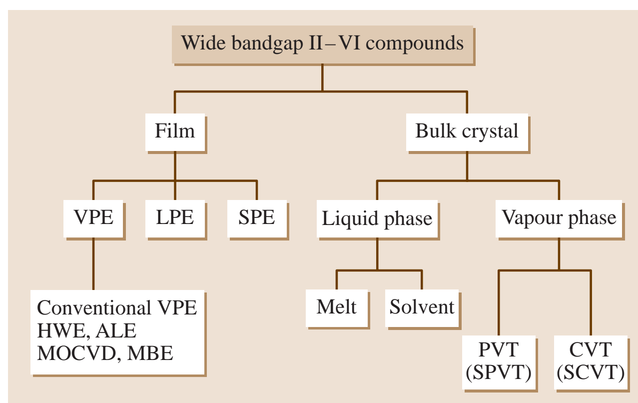

Fig. 16.2 Film and bulk-crystal growth techniques for II–VI wide-bandgap compounds

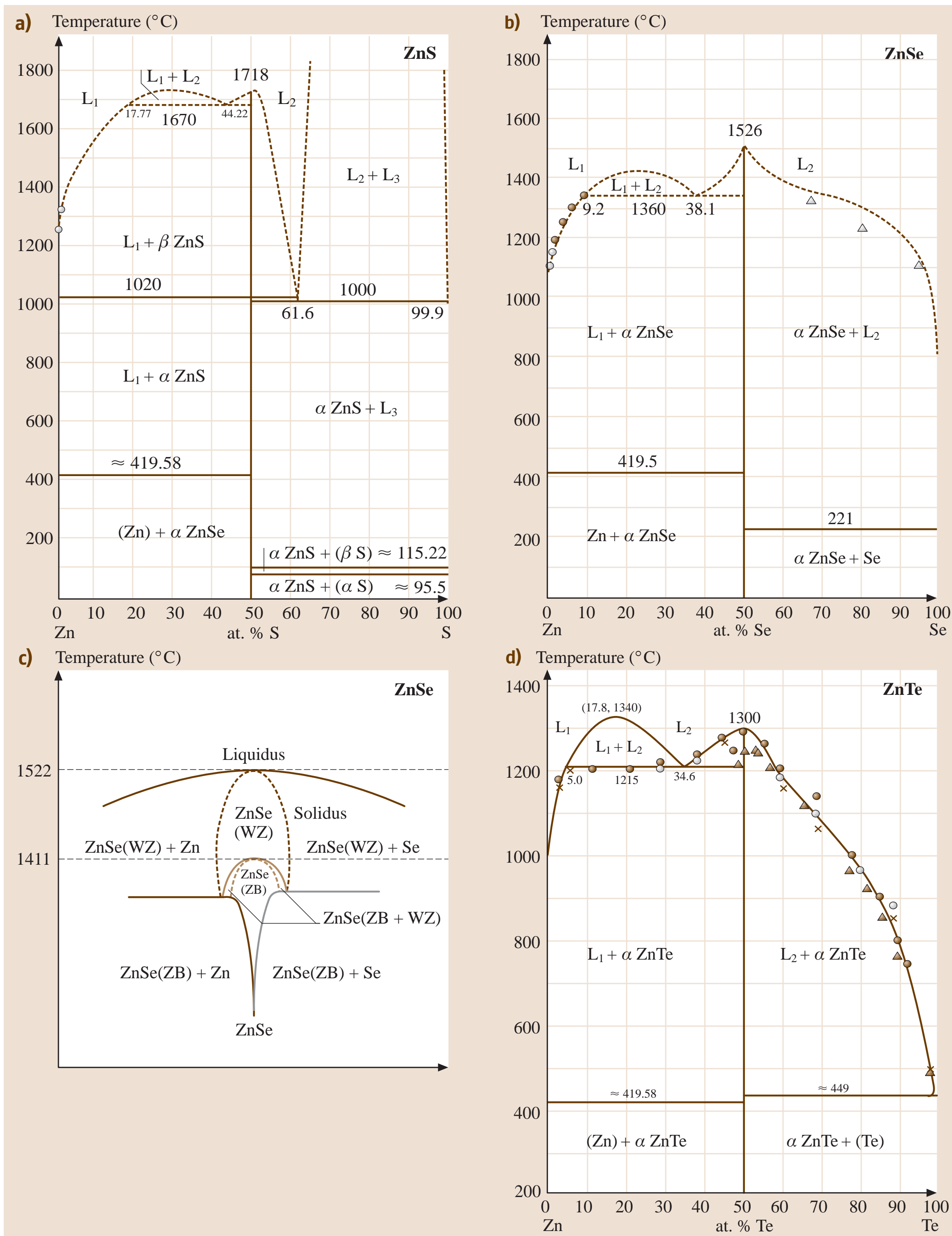
a) Temperature (°C)
ZnS
1800
1600
1400
1200
1000
800
600
400
200
L1 + L2
1718
L1
L2
17.77
1670
44.22
L2 + L3
L1 + β ZnS
1020
1000
61.6
99.9
L1 + α ZnS
α ZnS + L3
≈ 419.58
(Zn) + α ZnSe
α ZnS + (β S) ≈ 115.22
α ZnS + (α S) ≈ 95.5
0 10 20 30 40 50 60 70 80 90 100
Zn
at. % S
S
b) Temperature (°C)
ZnSe
1526
L1
L2
L1 + L2
9.2
1360
38.1
L1 + α ZnSe
α ZnSe + L2
419.5
221
Zn + α ZnSe
α ZnSe + Se
at. % Se
Se
c) Temperature (°C)
ZnSe
Liquidus
1522
1411
ZnSe (WZ)
Solidus
ZnSe(WZ) + Zn
ZnSe(WZ) + Se
ZnSe (ZB)
ZnSe(ZB + WZ)
ZnSe(ZB) + Zn
ZnSe(ZB) + Se
ZnSe
d) Temperature (°C)
ZnTe
(17.8, 1340)
1300
L1
L2
L1 + L2
5.0
1215
34.6
L1 + α ZnTe
L2 + α ZnTe
≈ 419.58
≈ 449
(Zn) + α ZnTe
α ZnTe + (Te)
at. % Te
Te

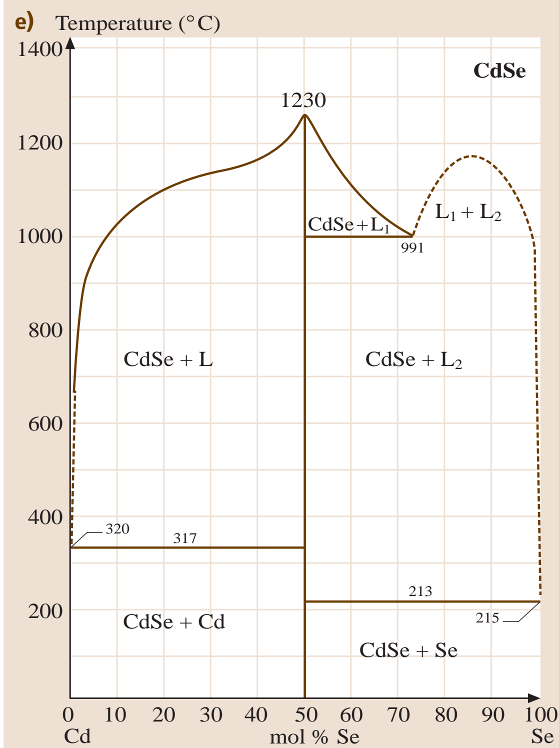

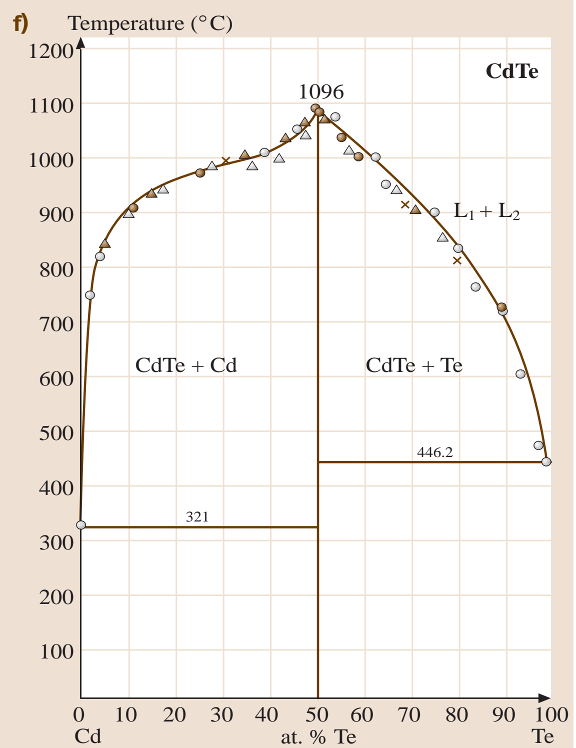

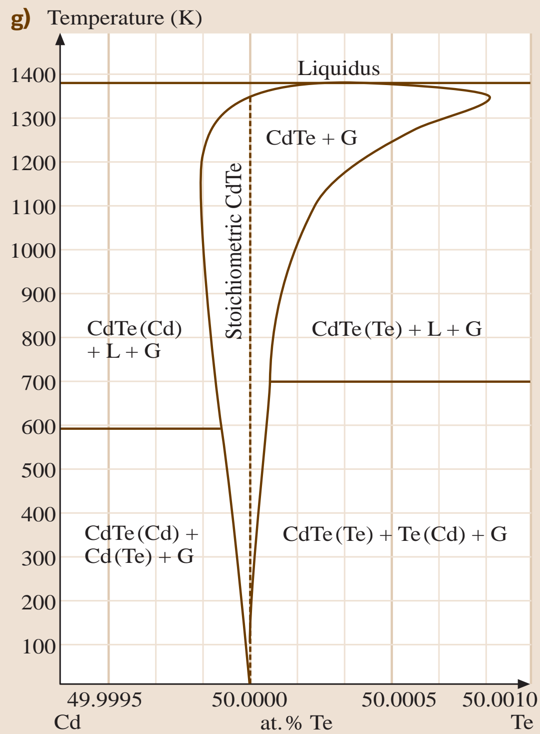

Fig. 16.3a–g Phase diagrams of some main wide-bandgap II–VI compounds. **(a)** ZnS, **(b)** ZnSe, **(c)** ZnSe phase diagram near the congruent point; **(d)** ZnTe; **(e)** CdSe; **(f)** CdTe; **(g)** CdTe phase diagram near the congruent point

16.1 Crystal Properties

16.1.1 Basic Properties

Wide-bandgap compound semiconductors have higher melting points. Due to their high ionicity, the overheating phenomenon occurs when they are heated to their melting point. Owing to the higher vapor pressures at their melting points, it is difficult to grow bulk crystals from melt. On the other hand, it is easy to grow bulk crystals as well as their films from the vapor phase. Therefore, before introducing film and bulk crystal growth, it is necessary to review their physical and chemical properties. Table 16.1 shows the properties of some of the main II–VI compound semiconductor materials [16.11–24].

16.1.2 Phase Diagram

It is necessary to understand the phase diagram to grow high-quality film and bulk single crystals. Figure 16.3 shows the phase diagrams reported for ZnS [16.25], ZnSe [16.25, 26], ZnTe [16.25], CdSe [16.27] and CdTe [16.28, 29]. Although much work has been done, there some exact thermodynamic data are still lacking, especially details close to the congruent point. Unfortunately, the phase diagram of ZnO is not available in spite of its growing importance in applications.

16.2 Epitaxial Growth

Epitaxial growth of wide-bandgap II–VI compounds was mainly carried out using liquid-phase epitaxy (LPE), or VPE. VPE includes several techniques, such as conventional VPE, hot-wall epitaxy (HWE), metalorganic chemical vapor deposition (MOCVD) or metalorganic phase epitaxy (MOVPE), molecular-beam epitaxy (MBE), metalorganic molecular-beam epitaxy (MOMBE) and atomic-layer epitaxy (ALE), etc. Each of these methods has its advantages and disadvantages. They are summarized in Table 16.2.

In the case of hetero-epitaxy, the mismatch between substrate material and epitaxial layer affects the growing structure and quality of the epitaxial layer. The mismatch should be made as small as possible when choosing the pair of materials (substrate and epitaxial material). Furthermore, the difference between the thermal expansion coefficients of the pair of materials has to be considered to obtain high-quality epitaxial layer [16.30].

16.2.1 The LPE Technique

LPE growth occurs at near-thermodynamic-equilibrium conditions. There are two growth methods. The first is called equilibrium cooling, in which the saturated solution is in contact with the substrate and the temperature is lowered slowly, the solution becomes supersaturated; meanwhile a slow epitaxial growth on the substrate is initiated. The second is the step-cooling process ,in which the saturated solution is cooled down a few degrees (5−20 K) to obtain a supersaturated solution. The substrate is inserted into the solution, which is kept at this cooled temperature. Growth occurs first due to the supersaturation, and will slow down and stop finally. For both techniques, if the substrate is dipped in sequence into several different melt sources, multiple layer structures can be grown. LPE can successfully and inexpensively grow homo- and heterostructures. As the growth is carried out under thermal equilibrium, an epilayer with a very low native defect density can be obtained.

The LPE method can be used to grow high-quality epilayers, such as ZnS [16.31], ZnSe [16.31, 32], ZnSSe [16.33], ZnTe [16.34], etc. *Werkhoven* et al. [16.32] grew ZnSe epilayers by LPE on ZnSe substrates in a low-contamination-level environment. In their study, the width of bound exciton lines in low-temperature photoluminescence spectra was used to define the quality of the material, and the energy of the lines was used to identify trace impurities. The photoluminescence (PL) results showed that the ZnSe epitaxial layer has the high quality. The sharpest spectra occurred in layers grown rapidly on a previously grown buffer layer, indicating the importance of impurity out-diffusion from the substrate into the growing layer. The sharpness of these bound exciton lines indicates that the total concentration of electrically active impurities ($N_A + N_D$) was below $10^{17}\,cm^{-3}$.

16.2.2 Vapor-Phase Epitaxy Techniques

Conventional VPE

A typical VPE growth system is shown in Fig. 16.4. In VPE growth, thin films are formed by the deposition of

Table 16.2 Strengths and weaknesses of several epitaxial growth techniques

LPE	Thermodynamic equilibrium growth Easy-to-use materials Low-temperature growth High purity Multiple layers Thickness control not very precise Poor surface/interface morphology	**MOCVD**	Gaseous reaction for deposition Precise composition Patterned/localized growth Potentially easier large-area multiple-wafer scale-up Low-temperature growth High-vapor-pressure materials growth allowed About 1 ML/s deposition rate Expensive equipment Safety precautions needed
HWE	Easy-to-use materials Low cost Thermodynamic equilibrium Hard to grow thick layers Thickness control not very precise	**MBE and MOMBE**	Physical vapor deposition Ultra-high-vacuum environment About 1 ML/s deposition rate In situ growth-front monitoring Precise composition Low growth rate Sophisticated equipment Limit for high-vapor-pressure materials growth (MBE)
VPE	Easy to operate Economic Thinner layers High growth rates Easier composition control High temperature (800–1000 °C)		
ALE	Gaseous reaction for deposition Low-temperature growth Precise composition Low growth rate Safety precautions needed		

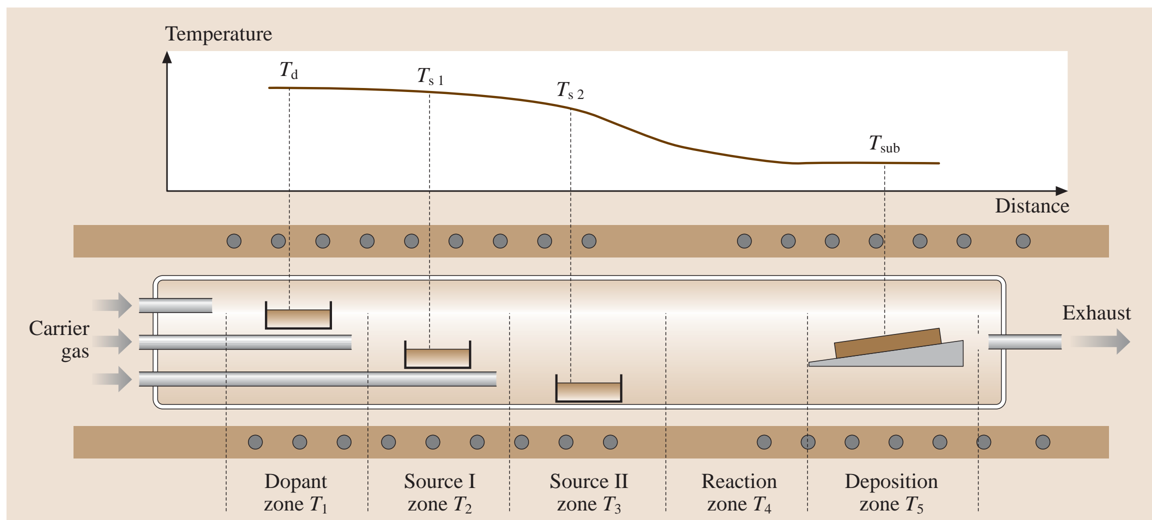

Fig. 16.4 A typical VPE growth system

atoms from the vapor phase. There are two types of transport mechanisms for the source materials, physical vapor deposition (PVD) without any chemical reaction, and chemical vapor deposition (CVD), where the formation of the deposited film is the result of a chemical reaction of the precursors on the substrate. In VPE growth, there are several important parameters, such as the source temperature, the substrate temperature, the flow rate of the carrier gas, the growth pressure, and so on. These determine the growth rate, composition, and crystallinity of the epitaxial layers.

The VPE technique is the most popular in semiconductor epitaxial growth. Since the vapor pressures of all wide-bandgap II–VI materials are high, their epitaxial layers can be grown by this method. As an example, high-quality ZnS single-crystal films have been grown on a Si substrate using hydrogen as a carrier gas [16.35, 36]. Furthermore, the Iida group [16.37] doped N and P into a ZnS epilayer and studied their behavior in details. The N and P were expected to compensate the native donor state and to result in an insulating material. The results showed that the doped acceptors N and P reduced the donor density and an insulating material was obtained. Later, this group was successful in preparing a p-type ZnS epilayer using NH_3 as an acceptor dopant [16.38]. Many efforts have been made to grow ZnSe epilayers on different substrates, especially on GaAs in the past two decades [16.39, 40]. p-type ZnSe was also obtained by this technique [16.41]. In addition, other compounds, ZnTe [16.42], CdS [16.43], CdSe [16.44], and CdTe [16.45], were also studied using this technique.

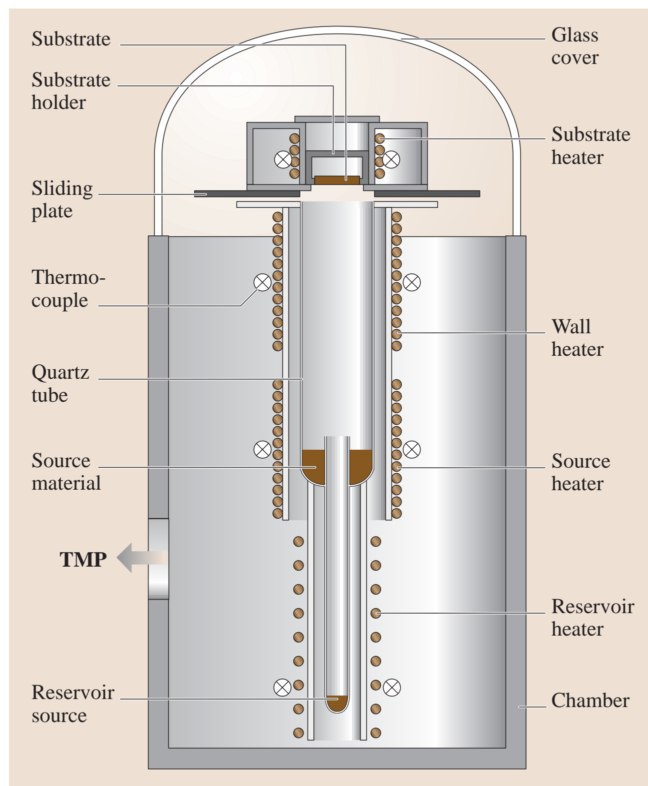

Fig. 16.5 Diagram of a typical HWE system growth chamber

The HWE Technique

Hot-wall epitaxy [16.1] has proved to be a very successful growth method for II–VI compound epitaxial layers. Its principal characteristic is the growth of thin films under conditions near thermodynamic equilibrium. Compared with other VPE methods, the HWE technique has the advantages of low cost, simplicity, convenience, and relatively high growth rate. In particular, it can control deviation from stoichiometry during growth of an epilayer.

A schematic diagram of the improved HWE system is showed in Fig. 16.5; it consists of four independent furnaces. The source material placed at the middle is transported to the substrate. The region of the growth reactor between the source and substrate, called the hot wall, guarantees a nearly uniform and isotropic flux of molecules onto the substrate surface. To control the deviation from stoichiometry, the reservoir part is placed at the bottom with a constituent element.

HWE has been applied to growing II–VI compound epilayers, such as CdTe [16.46], CdS [16.47], CdSe [16.48], ZnTe [16.49], and also to producing heterostructures for laser and photovoltaic detector fabrication [16.50]. Most research using HWE technique has focused on CdTe growth. *Wang* et al. [16.46] optimized growth conditions and grew high-quality CdTe epitaxial films using the HWE apparatus shown in Fig. 16.5. All the CdTe epilayers show mirror-like surfaces. Results from PL and X-ray diffraction (XRD) show that CdTe epilayers on GaAs suffer from a biaxial compressive stress, that this stress is rapidly relaxed within a thickness of about 5 μm, and that it remains in the epilayer up to a film thickness of 15 μm. Although this heterosystem has a 14.6% lattice mismatch and −26% thermal expansion mismatch at 300 K, high-quality CdTe epilayers, with a full-width half-maximum (FWHM) of 0.26 meV for bound-exciton emission lines in 4.2-K PL, about 90 arcs for (400) diffraction in four-crystal XRD spectrum, were prepared by selecting suitable growth conditions and epilayer thickness.

Recently, significant results have been achieved for CdTe/Si (111) epilayer growth by HWE. *Lalev* et al. [16.51] reported that high-quality CdTe (111) epilayers with *A* polarity were directly grown on hydrogen-terminated Si (111) without any preheating treatment. Through the originally designed two-step growth regime, the crystal quality of CdTe film was significantly improved, and the best FWHM value of 118 arcs from four-crystal rocking curves was obtained for a 5-μm-thick epilayer.

The MOCVD Technique

MOCVD or MOVPE is an improvement over conventional VPE. Since its introduction in 1968 [16.52], this technique has been established as one of the techniques for epitaxial growth of compound semiconductors both for research and production. The factors that have allowed MOCVD to reach this popularity are the purity and abruptness of the grown layers together with the flexibility of the technique, which makes the growth of almost all compound semiconductors possible. This abrupt transition in the composition of the epitaxial structure is necessary for the fabrication of digital or analog alloy system.

The development history of MOCVD technique is equivalent to that of source precursors. Since ZnSe epilayers were grown by MOCVD [16.52], many source precursors of II–VI elements have been developed. $Zn(CH_3)_2$ dimethylzinc (DMZn) and $Zn(C_2H_5)_2$ diethylzinc (DEZ) were used at the beginning of MOCVD growth [16.53]. ZnSe and ZnS films were grown using these metalorganic sources and inorganic H_2Se or H_2S. Unfortunately, the quality of these films was very poor. For this reason, $Se(CH_3)_2$ dimethylselenide (DMSe) and $Se(C_2H_5)_2$ diethylselenium (DESe) were developed [16.54]. The quality of epilayers was greatly improved. From then, II and VI elemental gas precursors were proposed one after another. *Wright* et al. grew a ZnSe film using ($DMZn-(NEt_3)_2$) triethylamine adduct of dimethylzinc [16.55]. *Hirata* et al. [16.56] and *Nishimura* et al. [16.57] proposed methylselenol (MSeH) and tertiarybutylselenol (*t*-BuSeH) as Se sources, respectively. Methylallylselenide (MASe) [16.58], diallyl-selenide (DASe) [16.59], t-butylallylselenide (*t*-BuASe) [16.60], tertiarybutyl-selenide (*Dt*-BuSe) [16.61], were also used as Se sources. *Fujita* et al. found methylmercaptan (MSH) as an S source [16.53]. Besides these, many other source precursors of II–VI elements, such as $Cd(CH_3)_2$ dimethylcadmium (DMCd) [16.62], $Te(CH_3)_2$ dimethyltelluride (DMTe) [16.62], $Te(C_2H_5)_2$ diethyltelluride (DETe), $Te(C_3H_7)_2$ diisopropyltelluride (DIPTe) [16.63], $S(C_2H_5)_2$ diethylsulfide (DES), $S(C_4H_9)_2$ ditertiarybutylsulfide (DTBS), $(C_4H_9)SH$ tertiarybutylthiol (tBuSH), have been used.

The great advantage of using metalorganics is that they are volatile at moderately low temperatures. Since all constituents are in the vapor phase, precise electronic control of gas flow rates and partial pressures is possible. This, combined with pyrolysis reactions that are relatively insensitive to temperature, allows efficient and reproducible deposition.

The substrate wafer is placed on a graphite susceptor inside a reaction vessel and heated by a radio-frequency (RF) induction heater. The growth temperature depends on the type of compounds grown. Growth is carried out in a hydrogen atmosphere at a pressure of 100–700 torr. The growth precursors decompose on contact with the hot substrate to form epitaxial layers. Each layer is formed by switching the source gases to yield the desired structure.

The films of almost all wide-bandgap II–VI compounds have been grown by MOCVD technique. Most work has been done on p-ZnSe epilayers in the past two decades [16.64–66]. The highest hole concentration of $8.8\times10^{17}\ cm^{-3}$ was reported with a NH_3 doping source [16.67]. Recently, quantum wells (QW) and quantum dots (QD) of these wide-bandgap compounds have become the focus. Successful pulsed laser operation at 77 K in ZnCdSe/ZnSe/ZnMgSSe QW-structure separated-confinement heterostructures has been realized [16.68].

MBE and MOMBE

MBE was developed at the beginning of the 1970s to grow high-purity high-quality compound semiconductor epitaxial layers on some substrates [16.69, 70]. To date, it has become a very important technique for growing almost all semiconductor epilayers. An MBE system is basically a vacuum evaporation apparatus. The pressure in the chamber is commonly kept below $\approx 10^{-11}$ torr. Any MBE process is dependent on the relation between the equilibrium vapor pressure of the constituent elements and that of the compound [16.71]. There are a number of features of MBE that are generally considered advantageous for growing semiconducting films: the growth temperature is relatively low, which minimizes any undesirable thermally activated processes such as diffusion; the epilayer thickness can be controlled precisely; and the introduction of different vapor species to modify the alloy composition and to control

the dopant concentration can be conveniently achieved by adding different beam cells with proper shutters. These features become particularly important in making structures involving junctions.

Metalorganic molecular-beam epitaxy growth (MOMBE) is one of the variations of the MBE system [16.72, 73]. The difference is that metalorganic gaseous sources are used as the source materials. Therefore, this growth technique has the merits of MOCVD and MBE.

MBE or MOMBE techniques have been used to grow epilayers of almost all wide-bandgap II–VI semiconductors [16.74,75]. Due to its features, it is very successful in growing super-thin layers, such as single quantum wells (SQW), multiple quantum wells (MQW) [16.76,77] and nanostructures [16.78].

In nanostructures, quantum dot (QD) structures have attracted a lot of attention in recent years. This field represents one of the most rapidly developing areas of current semiconductor. They present the utmost challenge to semiconductor technology, rendering possible fascinating novel devices. QD are nanometer-size semiconductor structures where charge carriers are confined in all three spatial dimensions. They are neither atomic nor bulk semiconductor, but may best be described as artificial atoms.

In the case of heteroepitaxial growth there are three different growth modes [16.79]: (a) Frank–van der Merwe (FM) or layer-by-layer growth, (b) Volmer–Weber (VW) or island growth, and (c) Stranski–Krastanov (SK) or layer-plus-island growth. Which growth mode will be adopted in a given system depends on the surface free energy of the substrate, (σ_s), that of the film, (σ_f), and the interfacial energy (σ_i). Layer-by-layer growth mode occurs when $\Delta\sigma = \sigma_f + \sigma_i - \sigma_s = 0$. The condition for FM-mode growth is rigorously fulfilled only for homoepitaxy, where $\sigma_s = \sigma_f$ and $\sigma_i = 0$. If the FM-mode growth condition is not fulfilled, then three-dimensional crystals form immediately on the substrate (VW mode). For a system with $\Delta\sigma = 0$ but with a large lattice mismatch between the substrate and the film, initial growth is layer-by-layer. However, the film is strained. As the film grows, the stored strain energy increases. This strained epilayer system can lower its total energy by forming isolated thick islands in which the strain is relaxed by interfacial misfit dislocations, which leads to SK growth in these strained systems. The SK growth mode occurs when there is a lattice mismatch between the substrate and the epilayer, causing the epilayer to be strained, which results in the growth of dot-like self-assembled islands. Wire-like islands can grow from dot-like islands via a shape transition which helps strain relaxation.

For nanostructure fabrication, a thin epilayer is usually grown on a substrate. This two-dimensional (2-D) layer is used to fabricate lower-dimensional structures such as wires (1-D) or dots (0-D) by lithographic techniques. However, structures smaller than the limits of conventional lithography techniques can only be obtained by self-assembled growth utilizing the principles of SK or VW growth. For appropriate growth conditions, self-assembled epitaxial islands can be grown in reasonably well-controlled sizes [16.80].

Because wide-bandgap II–VI materials typically have stronger exciton–phonon interactions than III–V materials, their nanostructures are expected to be very useful in fabricating optoelectronics devices and in exploring the exciton nature in low-dimensional structure. Self-assembled semiconductor nanostructures of different system, such as CdSe/ZnSe [16.81], ZnSe/ZnS [16.82], CdTe/ZnTe [16.83], CdS/ZnSe [16.84], are thought to be advantageous for future application. MBE/MOMBE [16.81, 84], MOCVD [16.82], HWE [16.85] are the main growth techniques used to obtain such structures. MBE is the most advanced technique for the growth of controlled epitaxial layers. With the advancement of nanoscience and nanotechnology, lower-dimensional nanostructures are being fabricated by lithographic techniques from two-dimensional epitaxial layers. Alternately, self-assembled, lower-dimensional nanostructures can be fabricated directly by self-assembly during MBE growth.

Atomic-Layer Epitaxy

ALE is a chemical vapor deposition technique [16.5] where the precise control of the system parameters (pressure and temperature) causes the reaction of adsorption of the precursors to be self-limiting and to stop with the completion of a single atomic layer. The precursors are usually metalorganic molecules. The special feature of ALE is that the layer thickness per cycle is independent of subtle variations of the growth parameters. The growth rate is only dependent on the number of growth cycles and the lattice constant of the deposited material. The conditions for thickness uniformity are fulfilled when material flux on each surface unit is sufficient for monolayer saturation. In an ALE reactor, this means freedom in designing the precursor transport and its interaction with the substrates.

The advantages obtainable with ALE depend on the material to be processed and the type of application. In single-crystal epitaxy, ALE may be a way to obtain

a lower epitaxial crystal-growth temperature. It is also a method for making precise interfaces and material layers needed in superlattice structures and super-alloys. In thin-film applications, ALE allows excellent thickness uniformity over large areas. The process has primarily been developed for processing of compound materials. ALE is not only used to grow conventional thin films of II–VI wide-bandgap compounds [16.5,86,87], but is also a powerful method for the preparation of monolayers (ML) [16.88].

16.3 Bulk Crystal Growth

Bulk crystal is the most important subject studied in recent decades. The quality of bulk crystals is the most important aspect of electronic device design. To date, many growth methods have been developed to grow high-quality crystals. Significant improvements have been made in bulk crystal growth with regard to uniformity, reproducibility, thermal stability, diameter control, and impurity and dopant control. According to the phase balance, crystals can be grown from vapor phase, liquid (melt) phase, and solid phase.

16.3.1 The CVT and PVT Techniques

Crystal growth from the the vapor phase is the most basic method. It has advantages that growth can be performed at lower temperatures. This can prevent from phase transition and undesirable contamination. Therefore, this method has commonly been used to grow II–VI compound semiconductors.

Crystal growth techniques from the vapor phase can be divided into chemical vapor transport (CVT) and physical vapor transport (PVT). CVT is based on chemical transport reactions that occur in a closed ampoule having two different temperature zones. Figure 16.6 shows a typical schematic diagram of the CVT technique. In the high-temperature region, the source AB reacts with the transport agent X:

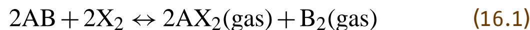

$$2AB + 2X_2 \leftrightarrow 2AX_2(gas) + B_2(gas) \quad (16.1)$$

In the low-temperature region, the reverse reaction takes place. The whole process continues by back-diffusion of the X_2 generated in the lower-temperature region. The transport agent X usually employed is hydrogen (H_2), a halogen (I_2, Br_2, Cl_2), a halide (HCl, HBr), and so on. For example, I_2 has been used as a transport agent for ZnS, ZnSe, ZnTe and CdS [16.89]; HCl, H_2, Cl_2, NH_3 [16.90], and C and CH_4 [16.91] have been used as the transport agents for ZnO. According to [16.89]: the typical growth temperature for ZnS is 1073–1173 K, for ZnSe 1023–1073 K, for ZnTe 973–1073 K; ΔT is 5–50 K; the concentration of the transport agent is 0.5–5 mg/cm^3 of the ampoules vapor space; the aspect ratios are 5–17 at ampoule diameters of 10–20 mm. According to [16.91]: the growth temperature for ZnO is

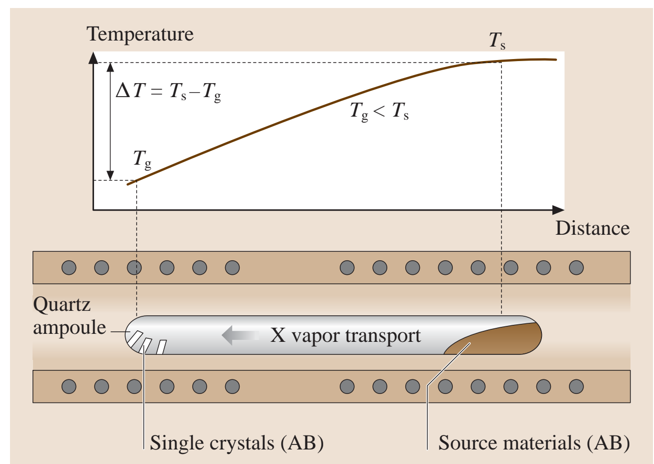

Fig. 16.6 Diagram of a conventional chemical vapor transport system

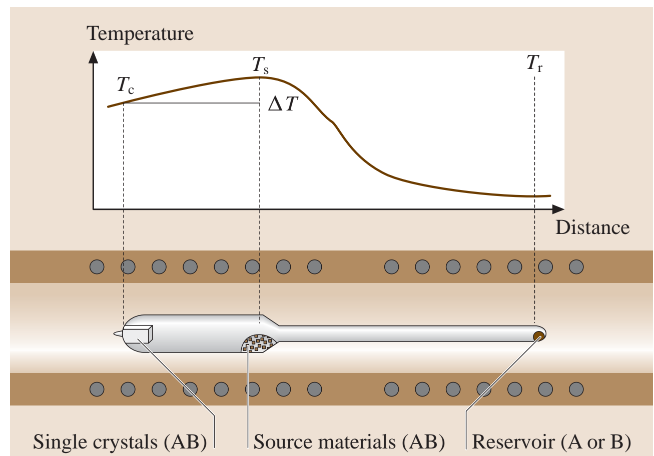

Fig. 16.7 Diagram of the physical vapor transport Piper–Polich method

1228–1273 K, and ΔT is 5–10 K. The transport rate does not strongly depend on the initial amount of carbon when the concentration of the transport agent is over 0.3 mg/cm^3.

The PVT method is similar to CVT, but the transport agent is not used. This technique is based on the dissociative sublimation of compounds. Initially, the Piper–Polich method was developed, in 1961 [16.92]. *Prior* [16.93] improved the PVT method using a reservoir to control the deviation from stoichiometry; the experimental arrangement is shown in Fig. 16.7. The constituent element is placed in the reservoir. The reservoir temperature can be calculated according to the solid–vapor equilibrium

$$2\mathrm{AB} \leftrightarrow 2\mathrm{A(gas)} + \mathrm{B_2(gas)}\,. \tag{16.2}$$

The total pressure (p) in ampoule is given by

$$\begin{aligned} p &= p_\mathrm{A} + p_{\mathrm{B}_2} \\ &= p_\mathrm{A} + K \cdot p_\mathrm{A}^{-2} \\ &= (K/p_{\mathrm{B}_2})^{1/2} + p_{\mathrm{B}_2}\,, \end{aligned} \tag{16.3}$$

where p_A and p_{B_2} are the partial pressures of the group II and VI elements respectively and $K = p_\mathrm{A}^{-2} \cdot p_{\mathrm{B}_2}$ is the equilibrium constant of (16.2). At any temperature, there is minimum total pressure (p_min), which corresponds to the condition,

$$p_\mathrm{A} = 2p_{\mathrm{B}_2} = 2^{1/3}K^{2/3}\,. \tag{16.4}$$

Under this condition, the vapor-phase composition is stoichiometric and growth rate is maximum [16.94]. After modifying this method to use a closed ampoule, it was applied to grow high-purity and high-quality crystals of II–VI compounds.

The PVT of II–VI compounds takes advantage of the volatility of both components of the compound semiconductor. This same volatility, coupled with typically high melting points, makes melt growth of these materials difficult. In the PVT process, an ampoule containing a polycrystalline source of the desired II–VI compound is heated to a temperature that causes the compound to sublime at a rate conducive to crystal growth. The ampoule is typically placed in a furnace having a temperature gradient over the length of the ampoule, so that the polycrystalline source materials sublime at the end with the higher temperature. The end of the ampoule where the crystal is to be grown is then maintained at a lower temperature. This temperature difference causes supersaturation, and vaporized molecules from source materials eventually deposit at the cooler end. In order to control the deviation from stoichiometry, a reservoir is often used (Fig. 16.7). One of the constituent elements is placed in it. By selecting the proper growth conditions, the rate of deposition can be set to a value leading to growth of high-quality crystals. Typically, PVT growth of II–VI compounds is carried out at temperatures much lower than their melting points; this gives benefits in terms of reduced defects, which are related to the melt growth of II–VI compounds such as voids and/or inclusions of excess components of the compound, and also helps to reduce the contamination of the growing crystal from the ampoule. Other effects, such as the reduction of point defects, are also typically found when crystals grown by PVT are compared to crystals grown by melt techniques. Although claims have been made that the lower temperatures of physical vapor transport crystal growth should also reduce the twinning found in most of the cubic II–VI compound crystals, the reduction is not usually realized in practice. The assumption that the twinning is a result of cubic/hexagonal phase transitions is not found to be the determining factor in twin formation.

Ohno et al. [16.95] grew cubic ZnS single crystals by the iodine transport method without a seed. By means of Zn-dip treatment, this low-resistivity crystal was used for homoepitaxial MOCVD growth, and a metal–insulator–semiconductor(MIS)-structured blue LED, which yielded an external quantum efficiency as high as 0.05%. They found that crystal quality was significantly improved by prebaking the ZnS powder in H_2S gas prior to growth. The growth rate also increased by three times.

Isshiki et al. [16.96] purified zinc by a process consisting of vacuum distillation and overlap zone melting in pure argon. Using refined zinc and commercial high-purity Se, high-quality ZnSe single crystals were grown by the same method, as reported by *Huang* and *Igaki* [16.97]. The emission intensities of donor-bound exciton (I_2) are remarkably small. The emission intensities of the radiative recombinations of free excitons (E_X) are very strong [16.98]. These intensities indicated the crystal had a very high purity and a very low donor concentration, and they suggest that the purity of the grown crystal strongly depends on the purity of the starting materials. This method is suitable for preparing high-purity crystals, since a purification effect is expected during growth. Impurities with a higher vapor pressure will condense at the reservoir portion and those with a lower vapor pressure will remain in the source crys-

tal. This effect was confirmed by the PL results [16.99]. As for these crystals, photoexcited cyclotron resonance measurements have been attempted and cyclotron resonance signals due to electrons [16.100] and heavy holes [16.101] have been detected for the first time. The cyclotron mobility of electrons under $B = 7\,\mathrm{T}$ is $2.3 \times 10^5\,\mathrm{cm^2/Vs}$. This indicates that the quality of the grown crystals is very high. Furthermore, the donor concentration in the crystal is estimated to be $4 \times 10^{14}\,\mathrm{cm^3}$ by analyzing the temperature dependence of the cyclotron mobility [16.99].

The crystals are grown in a self-seeded approach by the CVT or PVT techniques introduced above. This limits single-crystal volume to several $\mathrm{cm^3}$. Meanwhile, grain boundaries and twins are easy to form during growth. In order to solve these problems, seeded chemical vapor transport (SCVT) and seeded physical vapor transport (SPVT), the so-called modified Lely method, have been developed [16.102]. The difference between SCVT/SPVT and CVT/PVT is that a seed is set in the crystal growth space before growth starts. The most successful method of eliminating twin formation has usually been by using a polycrystal or single-crystal seed. Even this seeding cannot assure complete elimination of twinning unless seeding is done carefully. The usual method of using small seeds and increasing the diameter of the growing crystal are dependent on the preparation and condition of the walls of the ampoule and the furnace profiles required to eliminate spurious nucleation from the walls. Since the use of a seed crystal provides better control over the nucleation process, high-quality single crystals can be grown [16.103, 104]. Using this technique, sizable single crystals of II–VI wide-bandgap compounds has been commercialized.

Fujita et al. [16.105] grew ZnS single crystals as large as $24\,\mathrm{mm} \times 14\,\mathrm{mm} \times 14\,\mathrm{mm}$ by the SCVT method using iodine as a transport agent. The average linear growth rate was about $10^{-6}\,\mathrm{cm/s}$. The crystal size depended strongly on the ampoule geometry and the temperature difference between the seed and solvent. The study of the electrical properties showed that the annealed crystal was n-type.

16.3.2 Hydrothermal Growth

The hydrothermal technique is a method for growing crystal from aqueous solvent [16.106]. Figure 16.8 shows a diagram of hydrothermal techniques. The hydrothermal method of crystal growth has several advantages: (1) due to the use of a closed system, it is easier to control oxidization or maintain conditions that allow the synthesis of phases that are difficult to attain by other methods, such as compounds of elements in oxidation states, especially for transition-metal compounds; (2) crystal grow occurs under lower thermal strain, and thus may contain a lower dislocation density than when the crystal is grown from a melt, where large thermal gradients exist; (3) the method has proven to be very useful for the synthesis of the so-called low-temperature phases; (4) it can be employed for large-scale synthesis of piezoelectric, magnetic, optic, ceramic, and many other special materials; (5) hydrothermal synthesis results in rapid convection and very efficient solute transfer, which results in comparatively rapid growth of larger, purer, and dislocation-free crystals. The most successful example of obtaining II–VI compounds is growing single ZnO crystals.

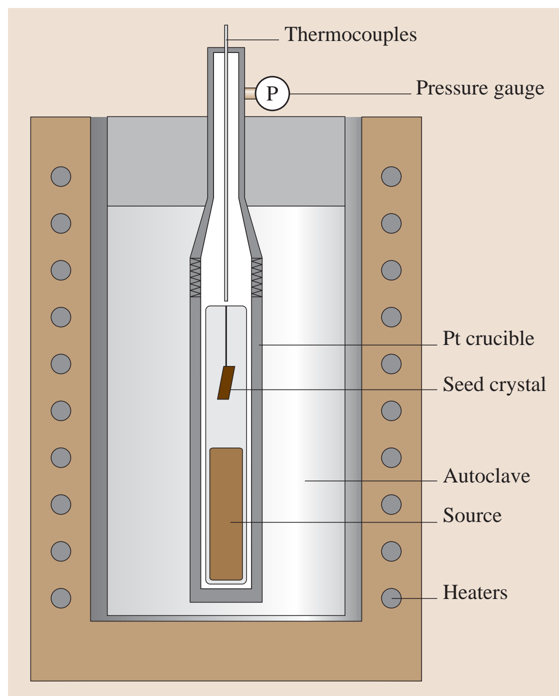

Fig. 16.8 Diagram of a typical hydrothermal technique for growing ZnO single crystals

ZnO crystals are considered extrinsic n-type piezoelectric semiconductors. Undoped crystals have a typical resistivity of $0.1–100\,\Omega\,\mathrm{cm}$ and a drift mobility of $10–125\,\mathrm{cm^2/Vs}$. Low carrier concentrations can be approached by special growth and annealing methods. ZnO crystal is quite transparent in the range $0.4–6.0\,\mu\mathrm{m}$. Slight absorption is sometimes found around $2.2–2.3\,\mu\mathrm{m}$ and an additional slight absorption

is found at 3.42 µm. Since 1953, *Walker* [16.107] and many other researchers [16.108–111] have grown large ZnO single crystals with hydrothermal techniques and other methods.

The seed, suspended by a Pt wire, and sintered ZnO strings as a source material (nutrient), together with a KOH (3M) and LiOH (1M) aqueous solution, were put into a Pt crucible [16.112] (the hydrothermal conditions are different in different papers). The seed crystals and the source material were separated by a Pt baffle. The crucible was sealed by welding and put into an autoclave. This hydrothermal autoclave is made of high-strength steel. Then, the autoclave was put into a vertical furnace. The temperature of the autoclave was raised to about 673 K, which produced 0.1 GPa of pressure. the growth temperature was monitored by a thermocouple inserted in the autoclave. Seed crystals grew to about 10 mm or bigger after two weeks. The crystal habit of hydrothermal ZnO crystals grown on basal plane seeds shows that growth direction in [0001] is faster 3 times than [000$\bar{1}$] [16.113].

16.3.3 Bridgman and Gradient Freezing (GF) Method

From the viewpoint of industrial production, melt growth is the most useful for obtaining large single crystals. VPE growth has limitations with regard to crystal size and productivity. The Bridgman technique is a typical crystal growth method from melt. Bridgman growth can be simply understood in terms of a molten charge that passes through a temperature gradient at a slow speed and solidifies when the temperature is below the melting point of this material. If the ampoule and furnace are stationary and the temperature is gradually reduced by keeping the temperature gradient at the

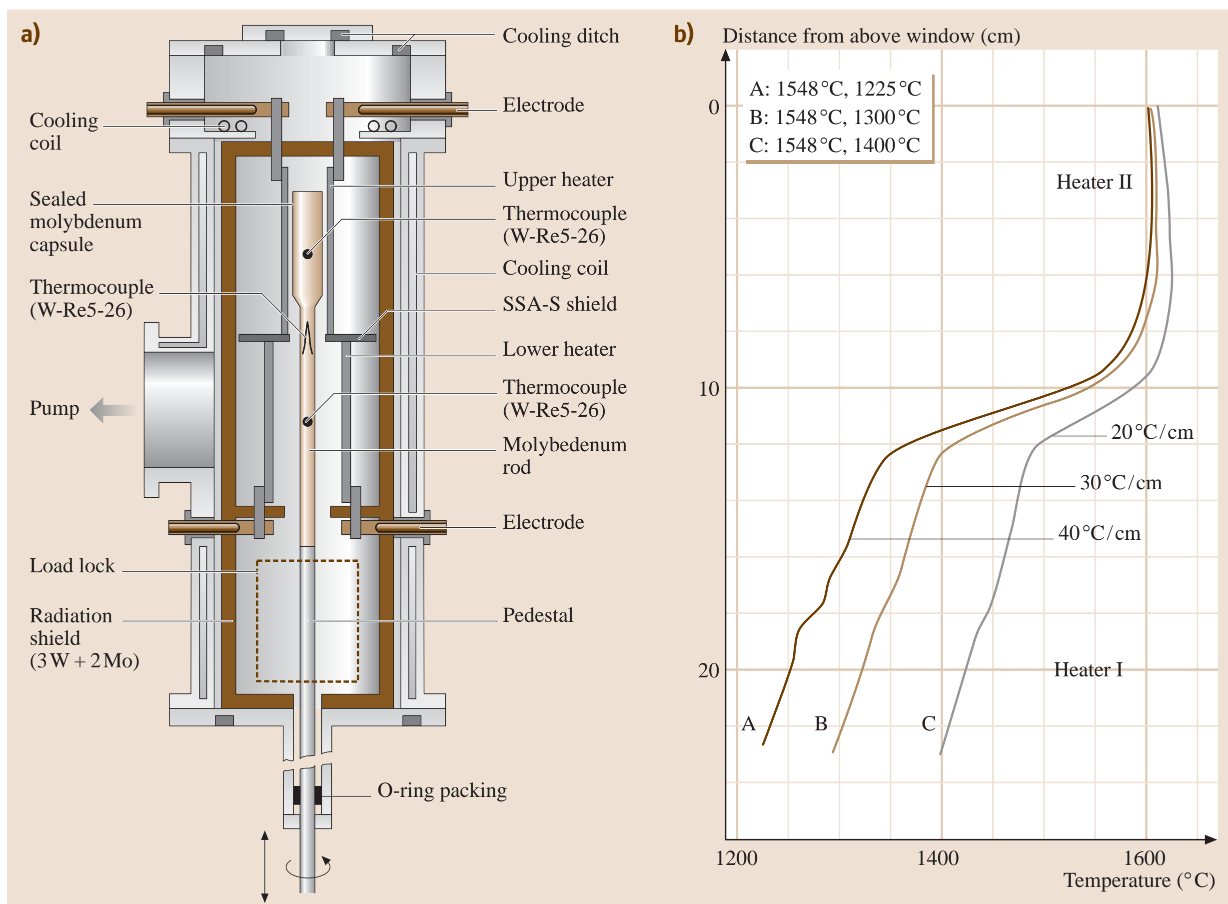

Fig. 16.9a,b Scheme of the vertical Bridgman growth system **(a)**, and its temperature profiles **(b)**

interface constant, this growth process is called the gradient freezing (GF) method [16.114]. In Bridgman or GF growth, single crystals can be grown using either seeded or unseeded ampoules or crucibles.

The Bridgman method has been most extensively used to grow II–VI wide-bandgap compounds such as CdTe, ZnTe and ZnSe crystals, because of the simplicity of the growth apparatus, the high growth rate and the availability of crystals of appropriate size and quality. There are two Bridgman method techniques: the high-pressure technique [16.115] and the closed technique [16.116]. In the former, it is inevitable that a compositional deviation from stoichiometry occurs during melting. Since the properties and structural perfection of these compound crystals are correlated very strongly with this nonstoichiometry [16.117], compositional deviation must be controlled during melt growth. *Omino* et al. [16.116] and *Wang* et al. [16.118, 119] have adopted a closed double crucible to prevent deviation of the melt from stoichiometric composition during Bridgman growth. Figure 16.9 shows a closed vertical Bridgman growth furnace and its temperature profiles.

In Bridgman growth, the temperature gradient (G) and growth rate (R) are very important parameters since they determine the shape of the solid–liquid interface. For this reason, the relationship between temperature gradient and growth rate is investigated. The experimental results are summarized in Fig. 16.10 [16.120, 121]. The experimental results show that, to grow a ZnSe single crystal, it is necessary that the G/R [(temperature) gradient/(growth) rate] value should be limited to $57{-}175\,\mathrm{K\,h/cm^2}$. The most suitable value of G/R, assessed from the determined optimum temperature gradient and growth rate, is $83\,\mathrm{K\,h/cm^2}$. *Wang* et al. [16.118, 119] found the optimum conditions to include: a special temperature program for removing the gas bubbles generated in melt, an overheating temperature of 76 K from the melting point of 1797 K, a temperature gradient of 30 K/cm and a growth rate of 3.6 mm/h as marked by the open squares in Fig. 16.10. Under these growth conditions, twin-free high-quality ZnSe single crystals (Fig. 16.11) were grown using a polycrystalline seed. Chemical etching on the cleaved (110) plane revealed that the average value of the etch pit density (EPD) is about $2\times10^5\,\mathrm{cm^{-2}}$. The rocking curves of four-crystal XRD showed a full-width at half-maximum (FWHM) value of 19 arcs. The resolved intensive free-exciton, bound-exciton emission lines and the weak donor-acceptor-pair (DAP) emission bands are observed in the PL spectra at 4.2 K. The FWHM of the I_1^{d} emission was smaller than 0.5 meV.

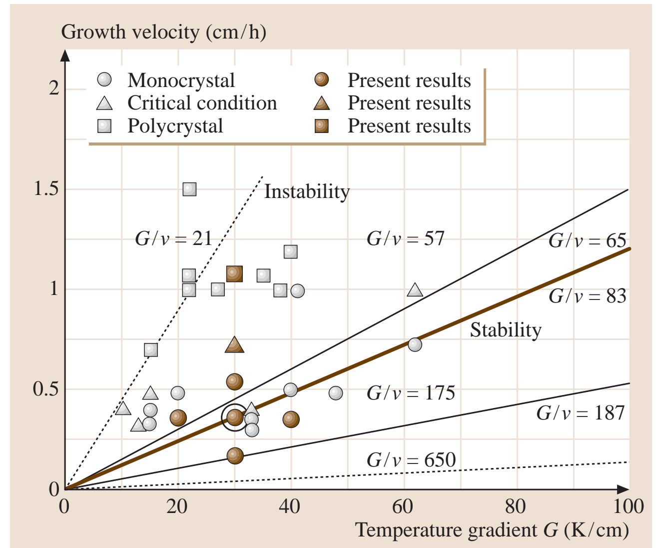

Fig. 16.10 Relationship between growth velocity and temperature gradient at the growth interfaces

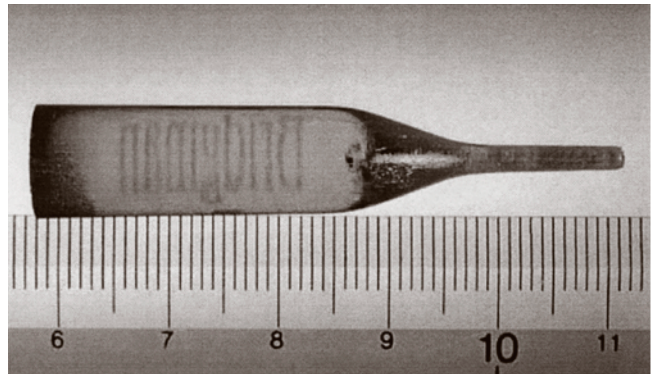

Fig. 16.11 Photograph of twin-free ZnSe single crystal grown by the vertical Bridgman technique

On the other hand, the deep-level emission bands were almost not observed. All these results suggest that the ZnSe single crystals grown by this method are of very high quality.

Asahi et al. [16.122] successfully grew ZnTe single crystals with a diameter of 80 mm and a length of 50 mm by the vertical gradient freezing (VGF) method. In this method, a high-pressure furnace was used and the melt was encapsulated by B_2O_3 during crystal growth. The growth direction was nearly ⟨111⟩ or ⟨110⟩. When long ZnTe crystals were grown, polycrystals were found at the tail. It seems to be difficult to grow an ingot longer than 50 mm. The researchers believed that this is because

Table 16.3 Growth methods for films and bulk crystals of wide-bandgap II–VI compounds

	Epitaxial growth						Bulk growth			
	LPE	VPE	HWE	ALE	MOCVD	MBE	CVT	PVT	Hydrothermal	Bridgman
ZnS	•	•		•	•	•	•	•		
ZnO					•	•	•		•	
ZnSe	•	•	•	•	•	•	•	•		•
ZnTe	•	•	•	•	•	•	•	•		•
CdS		•	•	•	•	•	•	•		•
CdSe		•	•	•	•	•	•	•		•
CdTe		•	•	•	•	•	•	•		•

the shape of the solid–liquid interface easily becomes concave against the liquid at the tail owing to the low thermal conductivity of ZnTe. Evaluation of the crystals showed that the FWHMs of the rocking curve measured by XRD were about 20 arcs, and the EPDs were $5\times10^{3}-1\times10^{4}\,cm^{-2}$.

16.3.4 The Traveling Heater Method (THM)

The traveling heater method (THM) [16.123] is a solution growth process whereby polycrystalline feed material with an average constant composition is progressively dissolved under the influence of a temperature gradient, followed by deposition in single-crystal form onto a seed with the same composition. The growth proceeds by the relative translation of the heater and charge. THM is particularly useful for the growth of binary and ternary semiconductor alloys, such as CdTe and CdZnTe [16.124]. In such materials, the wide separation between the solidus and liquidus in the pseudo-binary (CdTe–ZnTe) phase diagram imposes a monotonic variation in composition of the solid in the melt growth processes. The THM process ensures a constant macroscale composition in the crystal grown. Since the process takes place at a temperature below the melting point, contamination from the container is also reduced. The reduced operating temperature also leads to a lower ambient pressure within the growth environment, and a reduced risk of ampoule fracture.

16.3.5 Other Methods

Besides the growth methods described, there are many other techniques for growing single crystals of II–VI wide-bandgap compounds. Zone melting [16.125] and solid-state recrystallization (SSR) [16.126] are often used to grow bulk crystals of ZnSe, ZnS and CdTe.

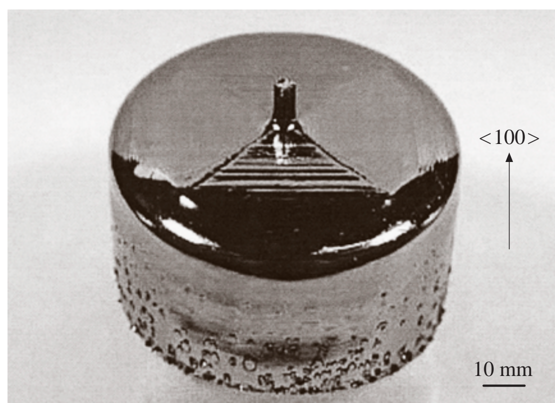

Fig. 16.12 ZnTe single crystal grown by a combination of the GF and Kyropoulos methods

Recently, *Asahi* et al. [16.127] proved that B_2O_3 is a suitable encapsulant for ZnTe melt growth. Furthermore, B_2O_3 and a total weight of 6N Zn and Te was charged into a pBN crucible. Then this crucible was put into a high-pressure furnace with five heaters. A ZnTe seed was used to pull the ZnTe crystal. Before growth started, the starting materials were heated to 1573 K and kept at this temperature for several hours. The pressure in the growth furnace was kept at 1.5–2 MPa using Ar gas during growth. The temperature gradient on the solid–liquid surface was about 10–20 K/cm. The growth rate was 2–4 mm/h. Under these growth conditions, ZnTe single crystals with a diameter of 80 mm and a height of 40 mm were successfully grown using a combined GF/Kyropoulos method [16.127] (Fig. 16.12).

Some growth methods for film and bulk crystals are summarized in Table 16.3.

16.4 Conclusions

It was expected that II–VI wide-bandgap compounds would become applicable to optoelectronic devices, especially LEDs and LDs in the short-wavelength visible-light region. However, as they are very strongly bonded with a nearly equal balance of covalent and ionic bonding, it is challenging to grow high-purity high-quality single crystals. Another problem with their application to devices is the difficulty of controlling the conductive type. This is because native defects commonly occur in these semiconductors. These native defects can have either a donor or acceptor character, or even be amphoteric, and they act as compensating centers. Furthermore, these defects react with dopant impurities to form complexes. This makes it difficult to reverse the conductive type. For example, in the case of ZnSe, it is still difficult to obtain low-resistivity p-type crystals or epilayers that can be used to fabricate devices. Therefore, a significant improvement in the understanding of the fundamental physical and chemical properties needs to be achieved. In particular, the specifications for many applications are very demanding, and considerable progress needs to be made in growth, particularly in the areas of reproducibility, convenient shape, conductivity, and structural perfection.

References

16.1 A. Lopez-Otero: Thin Solid Films **49**, 1 (1978)
16.2 H. M. Manasevit, W. I. Simpson: J. Electrochem. Soc. **118**, 644 (1971)
16.3 L. L. Chang, R. Ludeke: *Epitaxial Growth, Part A*, ed. by J. W. Matthews (Academic, New York 1975) p. 37
16.4 E. Veuhoff, W. Pletschen, P. Balk, H. Luth: J. Cryst. Growth **55**, 30 (1981)
16.5 T. Suntola: Mater. Sci. Rep. **4**, 261 (1989)
16.6 M. M. Faktor, R. Heckingbottom, I. Garrett: J. Cryst. Growth **9**, 3 (1971)
16.7 I. Kikuma, M. Furukoshi: J. Cryst. Growth **41**, 103 (1977)
16.8 Y. V. Korostelin, V. J. Kozlovskij, A. S. Nasibov, P. V. Shapkin: J. Cryst. Growth **159**, 181 (1996)
16.9 J. F. Wang, A. Omino, M. Isshiki: Mater. Sci. Eng. **83**, 185 (2001)
16.10 S. H. Song, J. F. Wang, G. M. Lalev, L. He, M. Isshiki: J. Cryst. Growth **252**, 102 (2003)
16.11 H. Harmann, R. Mach, B. Sell: In: *Current Topics Mater. Sci.*, Vol. 9, ed. by E. Kaldis (North-Holland, Amsterdam 1982) pp. 1–414
16.12 P. Rudolph, N. Schäfer, T. Fukuda: Mater. Sci. Eng. **15**, 85 (1995)
16.13 R. Shetty, R. Balasubramanian, W. R. Wilcox: J. Cryst. Growth **100**, 51 (1990)
16.14 K. W. Böer: *Survey of Semiconductor Physics, Vol. 1: Electrons and Other Particales in Bulk Semiconductors* (Van Nostrand, New York 1990)
16.15 C. M. Wolf, N. Holonyak, G. E. Stillman: *Physical Properties of Semiconductors* (Prentice Hall, New York 1989)
16.16 L. Smart, E. Moore: *Solid State Chemistry*, 2nd edn. (Chapman Hall, New York 1995)
16.17 E. Lide(Ed.): *Handbook of Chemistry and Physics*, 2nd edn. (CRC, Boca Raton 1973)
16.18 J. Singh: *Physics of Semiconductors and Their Heterostructures* (McGraw-Hill, New York 1993)
16.19 N. Yamamoto, H. Horinaka, T. Miyauchi: Jpn. J. Appl. Phys. **18**, 225 (1997)
16.20 H. Neumann: Kristall Technik **15**, 849 (1980)
16.21 J. Camassel, D. Auvergne, H. Mathieu: J. Phys. Colloq. **35**, C3-67 (1974)
16.22 W. Shan, J. J. Song, H. Luo, J. K. Furdyna: Phys. Rev. **50**, 8012 (1994)
16.23 K. A. Dmitrenko, S. G. Shevel, L. V. Taranenko, A. V. Marintchenko: Phys. Status Solidi B **134**, 605 (1986)
16.24 S. Logothetidis, M. Cardona, P. Lautenschlager, M. Garriga: Phys. Rev. B **34**, 2458 (1986)
16.25 R. C. Sharma, Y. A. Chang: J. Cryst. Growth **88**, 192 (1988)
16.26 H. Okada, T. Kawanaka, S. Ohmoto: J. Cryst. Growth **165**, 31 (1996)
16.27 N. Kh. Abrikosov, V. F. Bankina, L. B. Poretzkaya, E. V. Skudnova, S. N. Chichevskaya: *Poluprovodnikovye chalkogenidy i splavy na ikh osnovje* (Nauka, Moscow 1975) (in Russian)
16.28 R. F. Brebrick: J. Cryst. Growth **86**, 39 (1988)
16.29 M. R. Lorenz: *Physics and Chemistry of II–VI Compounds*, ed. by M. Aven, J. S. Prener (North Holland, Amsterdam 1967) pp. 210–211
16.30 T. Yao: Optoelectron. Dev. Technol. **6**, 37 (1991)
16.31 H. Nakamura, M. Aoki: Jpn. J. Appl. Phys. **20**, 11 (1981)
16.32 C. Werkhoven, B. J. Fitzpatrik, S. P. Herko, R. N. Bhargave, P. J. Dean: Appl. Phys. Lett. **38**, 540 (1981)
16.33 H. Nakamura, S. Kojima, M. Wasgiyama, M. Aoki: Jpn. J. Appl. Phys. **23**, L617 (1984)
16.34 V. M. Skobeeva, V. V. Serdyuk, L. N. Semenyuk, N. V. Malishin: J. Appl. Spectrosc. **44**, 164 (1986)
16.35 P. Lilley, P. L. Jones, C. N. W. Litting: J. Mater. Sci. **5**, 891 (1970)
16.36 T. Matsumoto, T. Morita, T. Ishida: J. Cryst. Growth **53**, 225 (1987)

16.37 S. Zhang, H. Kinto, T. Yatabe, S. Iida: J. Cryst. Growth **86**, 372 (1988)
16.38 S. Iida, T. Yatabe, H. Kinto: Jpn. J. Appl. Phys. **28**, L535 (1989)
16.39 P. Besomi, B.W. Wessels: J. Cryst. Growth **55**, 477 (1981)
16.40 T. Kyotani, M. Isshiki, K. Masumoto: J. Electrochem. Soc. **136**, 2376 (1989)
16.41 N. Stucheli, E. Bucher: J. Electron. Mater. **18**, 105 (1989)
16.42 M. Nishio, Y. Nakamura, H. Ogawa: Jpn. J. Appl. Phys. **22**, 1101 (1983)
16.43 N. Lovergine, R. Cingolani, A.M. Mancini, M. Ferrara: J. Cryst. Growth **118**, 304 (1992)
16.44 O. De. Melo, E. Sánchez, S. De. Roux, F. Rábago-Bernal: Mater. Chem. Phys., **59**, 120 (1999)
16.45 M. Kasuga, H. Futami, Y. Iba: J. Cryst. Growth **115**, 711 (1991)
16.46 J.F. Wang, K. Kikuchi, B.H. Koo, Y. Ishikawa, W. Uchida, M. Isshiki: J. Cryst. Growth **187**, 373 (1998)
16.47 J. Humenberger, G. Linnet, K. Lischka: Thin Solid Films **121**, 75 (1984)
16.48 F. Sasaki, T. Mishina, Y. Masumoto: J. Cryst. Growth **117**, 768 (1992)
16.49 B.J. Kim, J.F. Wang, Y. Ishikawa, S. Sato, M. Isshiki: Phys. Stat. Sol. (a) **191**, 161 (2002)
16.50 A. Rogalski, J. Piotrowski: Prog. Quantum Electron. **12**, 87 (1988)
16.51 G.M. Lalev, J. Wang, S. Abe, K. Masumoto, M. Isshiki: J. Crystal Growth **256**, 20 (2003)
16.52 H.M. Manasevit: Appl. Phys. Lett. **12**, 1530 (1968)
16.53 Sg. Fujita, M. Isemura, T. Sakamoto, N. Yoshimura: J. Cryst. Growth **86**, 263 (1988)
16.54 H. Mitsuhashi, I. Mitsuishi, H. Kukimoto: J. Cryst. Growth **77**, 219 (1986)
16.55 P.J. Wright, P.J. Parbrook, B. Cockayne, A.C. Jones, E.D. Orrell, K.P. O'Donnell, B. Henderson: J. Cryst. Growth **94**, 441 (1989)
16.56 S. Hirata, M. Isemura, Sz. Fujita, Sg. Fujita: J. Cryst. Growth **104**, 521 (1990)
16.57 S. Nishimura, N. Iwasa, M. Senoh, T. Mukai: Jpn. J. Appl. Phys. **32**, L425 (1993)
16.58 K.P. Giapis, K.F. Jensen, J.E. Potts, S.J. Pachuta: Appl. Phys. Lett. **55**, 463 (1989)
16.59 S.J. Pachuta, K.F. Jensen, S.P. Giapis: J. Cryst. Growth **107**, 390 (1991)
16.60 M. Danek, J.S. Huh, L. Foley, K.F. Jenson: J. Cryst. Growth **145**, 530 (1994)
16.61 W. Kuhn, A. Naumov, H. Stanzl, S. Bauer, K. Wolf, H.P. Wagner, W. Gebhardt, U.W. Pohl, A. Krost, W. Richter, U. Dümichen, K.H. Thiele: J. Cryst. Growth **123**, 605 (1992)
16.62 J.K. Menno, J.W. Kerri, F.H. Robert: J. Phys. Chem. B **101**, 4882 (1997)
16.63 H.P. Wagner, W. Kuhn, W. Gebhardt: J. Cryst. Growth **101**, 199 (1990)
16.64 N.R. Taskar, B.A. Khan, D.R. Dorman, K. Shahzad: Appl. Phys. Lett. **62**, 270 (1993)
16.65 Y. Fujita, T. Terada, T. Suzuki: Jpn. J. Appl. Phys. **34**, L1034 (1995)
16.66 J. Wang, T. Miki, A. Omino, K.S. Park, M. Isshiki: J. Cryst. Growth **221**, 393 (2000)
16.67 M.K. Lee, M.Y. Yeh, S.J. Guo, H.D. Huang: J. Appl. Phys. **75**, 7821 (1994)
16.68 A. Toda, T. Margalith, D. Imanishi, K. Yanashima, A. Ishibashi: Electron. Lett. **31**, 1921 (1995)
16.69 A. Cho: J. Vac. Sci. Tech. **8**, S31 (1971)
16.70 C.T. Foxon: J. Cryst. Growth **251**, 130 (2003)
16.71 T. Yao: *The Technology and Physics of Molecular Beam Epitaxy*, ed. by E.H.C. Parker (Plenum, New York 1985) Chap. 10, p. 313
16.72 E. Veuhoff, W. Pletschen, P. Balk, H. Luth: J. Cryst. Growth **55**, 30 (1981)
16.73 M.B. Panish, S. Sumski: J. Appl. Phys. **55**, 3571 (1984)
16.74 Y.P. Chen, G. Brill, N.K. Dhar: J. Cryst. Growth **252**, 270 (2003)
16.75 H. Kato, M. Sano, K. Miyamoto, T. Yao: J. Cryst. Growth **237–239**, 538 (2002)
16.76 M. Imaizumi, M. Adachi, Y. Fujii, Y. Hayashi, T. Soga, T. Jimbo, M. Umeno: J. Cryst. Growth **221**, 688 (2000)
16.77 W. Xie, D.C. Grillo, M. Kobayashi, R.L. Gunshor, G.C. Hua, N. Otsuka, H. Jeon, J. Ding, A.V. Nurmikko: Appl. Phys. Lett. **60**, 463 (1992)
16.78 S. Guha, A. Madhukar, K.C. Rajkumar: Appl. Phys. Lett. **57**, 2110 (1990)
16.79 E. Bauer, J.H. van der Merwe: Phys. Rev. B **33**, 3657 (1986)
16.80 J. Drucker, S. Chapparro: Appl. Phys. Lett. **71**, 614 (1997)
16.81 S.H. Xin, P.D. Wang, A. Yin, C. Kim, M. Dobrowolska, J.L. Merz, J.K. Furdyna: Appl. Phys. Lett. **69**, 3884 (1996)
16.82 M.C. Harris Liao, Y.H. Chang, Y.H. Chen, J.W. Hsu, J.M. Lin, W.C. Chou: Appl. Phys. Lett. **70**, 2256 (1997)
16.83 Y. Terai, S. Kuroda, K. Takita, T. Okuno, Y. Masumoto: Appl. Phys. Lett. **73**, 3757 (1998)
16.84 M. Kobayashi, S. Nakamura, K. Wakao, A. Yoshikawa, K. Takahashi: J. Vac. Sci. Technol. B **16**, 1316 (1998)
16.85 S.O. Ferreira, E.C. Paiva, G.N. Fontes, B.R.A. Neves: J. Appl. Phys. **93**, 1195 (2003)
16.86 M.A. Herman, J.T. Sadowski: Cryst. Res. Technol. **34**, 153 (1999)
16.87 M. Ahonen, M. Pessa, T. Suntola: Thin Solid Films **65**, 301 (1980)
16.88 M. Ritala, M. Leskelä: Nanotechnology **10**, 19 (1999)
16.89 H. Hartmann: J. Cryst. Growth **42**, 144 (1977)
16.90 M. Shiloh, J. Gutman: J. Cryst. Growth **11**, 105 (1971)
16.91 S. Hassani, A. Tromson-Carli, A. Lusson, G. Didier, R. Triboulet: Phys. Stat. Sol. (b) **229**, 835 (2002)
16.92 W.W. Piper, S.J. Polich: J. Appl. Phys. **32**, 1278 (1961)

16.93 A. C. Prior: J. Electrochem. Soc. **108**, 106 (1961)
16.94 T. Kiyosawa, K. Igaki, N. Ohashi: Trans. Jpn. Inst. Metala **13**, 248 (1972)
16.95 T. Ohno, K. Kurisu, T. Taguchi: J. Cryst. Growth **99**, 737 (1990)
16.96 M. Isshiki, T. Tomizono, T. Yoshita, T. Ohkawa, K. Igaki: J. Jpn. Inst. Metals **48**, 1176 (1984)
16.97 X. M. Huang, K. Igaki: J. Cryst. Growth **78**, 24 (1986)
16.98 M. Isshiki, T. Yoshita, K. Igaki, W. Uchida, S. Suto: J. Cryst. Growth **72**, 162 (1985)
16.99 M. Isshiki: J. Cryst. Growth **86**, 615 (1988)
16.100 T. Ohyama, E. Otsuka, T. Yoshita, M. Isshiki, K. Igaki: Jpn. J Appl. Phys. **23**, L382 (1984)
16.101 T. Ohyama, K. Sakakibara, E. Otsuka, M. Isshiki, K. Igaki: Phys. Rev. B **37**, 6153 (1988)
16.102 Y. M. Tairov, V. F. Tsvetkov: J. Cryst. Growth **43**, 209 (1978)
16.103 G. Cantwell, W. C. Harsch, H. L. Cotal, B. G. Markey, S. W. S. McKeever, J. E. Thomas: J. Appl. Phys. **71**, 2931 (1992)
16.104 Yu. V. Korostelin, V. I. Kozlovsky, A. S. Nasibov, P. V. Shapkin: J. Cryst. Growth **161**, 51 (1996)
16.105 S. Fujita, H. Mimoto, H. Takebe, T. Noguchi: J. Cryst. Growth **47**, 326 (1979)
16.106 K. Byrappa: *Hydrothermal Growth of Crystal*, ed. by K. Byrappa (Pergamon, Oxford 1991)
16.107 A. C. Walker: J. Am. Ceram. Soc. **36**, 250 (1953)
16.108 R. A. Laudice, E. D. Kolg, A. J. Caporaso: J. Am. Ceram. Soc. **47**, 9 (1964)
16.109 M. Suscavage, M. Harris, D. Bliss, P. Yip, S.-Q. Wang, D. Schwall, L. Bouthillette, J. Bailey, M. Callahan, D. C. Look, D. C. Reynolds, R. L. Jones, C. W. Litton: MRS Internet J. Nitride Semicond. Res **4S1**, G3.40 (1999)
16.110 L. N. Demianets, D. V. Kostomarov: Ann. Chim. Sci. Mater. **26**, 193 (2001)
16.111 N. Ohashi, T. Ohgaki, T. Nakata, T. Tsurumi, T. Sekiguchi, H. Haneda, J. Tanaka: J. Kor. Phys. Soc. **35**, S287 (1999)
16.112 D. C. Look, D. C. Reynolds, J. R. Sizelove, R. L. Jones, C. W. Litton, G. Gantwell, W. C. Harsch: Solid State Commun. **105**, 399 (1988)
16.113 T. Sekiguchi, S. Miyashita, K. Obara, T. Shishido, N. Sakagami: J. Cryst. Growth **214/215**, 72 (2000)
16.114 P. Höschl, Yu. M. Ivanov, E. Belas, J. Franc, R. Grill, D. Hlidek, P. Moravec, M. Zvara, H. Sitter, A. Toth: J. Cryst. Growth **184/185**, 1039 (1998)
16.115 T. Fukuda, K. Umetsu, P. Rudolph, H. J. Koh, S. Iida, H. Uchiki, N. Tsuboi: J. Cryst. Growth **161**, 45 (1996)
16.116 A. Omino, T. Suzuki: J. Cryst. Growth **117**, 80 (1992)
16.117 I. Kikuma, M. Furukoshi: J. Cryst. Growth **71**, 136 (1985)
16.118 J. F. Wang, A. Omino, M. Isshiki: J. Cryst. Growth **214/215**, 875 (2000)
16.119 J. Wang, A. Omino, M. Isshiki: J. Cryst. Growth **229**, 69 (2001)
16.120 J. F. Wang, A. Omino, M. Isshiki: Mater. Sci. Eng. B **83**, 185 (2001)
16.121 P. Rudolph, N. Schäfer, T. Fukuda: Mater. Sci. Eng. R **15**, 85 (1995)
16.122 T. Asahi, A. Arakawa, K. Sato: J. Cryst. Growth **229**, 74 (2001)
16.123 M. Ohmori, Y. Iwase, R. Ohno: Mater. Sci. Eng. B **16**, 283 (1999)
16.124 R. Triboulet: Prog. Cryst. Growth Char. Mater. **128**, 85 (1994)
16.125 H. H. Woodbury, R. S. Lewandowski: J. Cryst. Growth **10**, 6 (1971)
16.126 R. Triboulet: Cryst. Res. Technol. **38**, 215 (2003)
16.127 T. Asahi, T. Yabe, K. Sato: The Japan Society of Applied Physics and Related Societies, Extended Abstracts, The 50th Spring Meeting, (2003) p. 332